Skeletal Radiology
https://doi.org/10.1007/s00256-026-05414-w

SCIENTIFIC ARTICLE

Temporal MRI appearance of postoperative healing after proximal hamstring musculotendinous complex repair

Sandra Mechó[1,2,3] · Pamela Pérez[4] · Alejandro Congo[2] · Jaime Isern-Kebschull[5] · Xavier Alomar[3] · Ricard Pruna[1] · Xavi Valle[6] · Xavi Yanguas[1] · Ignasi Moix[1] · Jordi Puigdellívol[1] · Lasse Lempainen[7] · Marc Aguilar[1] · Carles Pedret[8] · Ara Kassarjian[9,10] · Gil Rodas[1]

Received: 3 August 2026 / Revised: 8 October 2026 / Accepted: 22 October 2026
© The Author(s), under exclusive licence to International Skeletal Society (ISS) 2026

Abstract

Objective To describe the temporal MRI features of healing during the first 4 months following surgical repair of complete tears of the proximal hamstring musculotendinous complex.

Materials and methods Consecutive case series. Professional football players with MRI-confirmed complete tears surgically repaired between May 2017 and December 2025 were retrospectively identified. Postoperative MRI examinations were obtained during routine clinical follow-up using 3-T systems. Two musculoskeletal radiologists independently evaluated longitudinal and transverse intratendinous clefts, scar maturation, edema-like signal, postoperative subcutaneous soft-tissue signal change, tendinous angulation, blunt muscle outline, and denervation-like signal.

Results Twenty-four complete tears in 20 players underwent surgical repair. Fifteen tendons with an uncomplicated postoperative course comprised the primary descriptive cohort, yielding 43 MRI examinations. Longitudinal intratendinous clefts were observed in 11/15 (73.3%) of tendons, transverse intratendinous clefts in 13/15 (86.7%), postoperative subcutaneous soft-tissue signal change and tendinous angulation in 15/15 (100%), blunt muscle outline in 13/15 (86.7%), and denervation-like signal in 10/15 (66.7%). In the within-tendon analysis, longitudinal and transverse intratendinous clefts resolved by the last available MRI in 6/10 (60%) and 7/12 (58.3%) tendons, respectively. All 10 tendons with an initially immature scar progressed to a mature scar. Among six tendons with postoperative exacerbation, four showed extensive, prominent intratendinous clefts with marked PD-FS hyperintensity on the preceding MRI, associated with immature scar, intratendinous cavity, or persistent interstitial edema-like signal.

Conclusion Serial MRI demonstrated different temporal patterns of postoperative healing. Residual intratendinous clefts may coexist with a mature scar during tendon remodeling and do not necessarily indicate delayed healing.

Keywords Proximal hamstring tendon repair · MRI · Tendon healing · Postoperative imaging · Hamstring injuries

Carles Pedret, Ara Kassarjian, and Gil Rodas contributed equally as senior authors.

✉ Sandra Mechó
mechomeca@gmail.com

1 FC Barcelona Medical Department (FIFA Medical Center of Excellence), and Barça Innovation Hub, Health & Wellness Area, Barcelona, Spain

2 Department of Radiology, Hospital of Barcelona, Diagonal Ave 660, Barcelona 08034, Spain

3 Department of Radiology, Centres Mèdics Creu Blanca, Barcelona, Spain

4 Department of Radiology, CAP Sant Felix, Sabadell, Spain

5 Department of Radiology, Hospital Clinic Barcelona, Barcelona, Spain

6 Sports Medicine Unit, ICATME-DEXEUS, Barcelona, Spain

7 FinnOrthopaedics, Hospital Pihlajalinna, Turku, Finland

8 Sports Medicine and Imaging Department, Clínica Diagonal, Esplugues de Llobregat, Spain

9 Elite Sports Imaging, SL, Madrid, Spain

10 Olympia Medical-Surgical Center, Madrid, Spain

Published online: 30 October 2026

Introduction

Hamstring injuries are the most common muscle injuries in running-based sports, particularly football, rugby, and athletics [1, 2]. In European football, the proportion of injuries diagnosed as hamstring injuries has increased from 12 to 24% over 21 seasons, and their contribution to all injury-related absence days has risen from 10 to 20%. Notably, about 18% of all reported hamstring injuries were recurrences [3]. The long head of the biceps femoris (LhBF) is the most commonly affected muscle (24% incidence) [4], with proximal injuries being the most prevalent and associated with longer recovery times and higher reinjury risk [5–7]. A complete tear of the proximal free tendon of the long head of the biceps femoris (LhBF) and semitendinosus (ST) represents the most severe hamstring injury in athletes [8]. The proximal musculotendinous complex of the long head of the biceps femoris comprises the proximal free tendon and the proximal common aponeurosis, both of which share fibers with the semitendinosus, and the intramuscular aponeurosis, which is specific to the LhBF (Fig. 1). Throughout this manuscript, the term "proximal common aponeurosis" refers to the aponeurotic segment located between the free tendon and the intramuscular aponeurosis. The semimembranosus tendon represents a separate component of the proximal hamstring complex and may also be involved in proximal hamstring injuries, either in isolation or in association with injuries of the long head of the biceps femoris–semitendinosus complex. However, the present study specifically focuses on surgically treated complete tears of the long head of the biceps femoris–semitendinosus proximal musculotendinous complex.

Sprint-related hamstring injuries involve different anatomical components depending on age [7]. In adolescents and young athletes, sprinting injuries more frequently involve the proximal free tendon, whereas in skeletally mature adults they predominantly affect the proximal aponeurosis of the long head of the biceps femoris. Consequently, complete tears of the proximal hamstring musculotendinous complex represent a characteristic injury pattern in young high-level athletes, particularly in sports requiring maximal sprinting.

The optimal management of complete tears of the proximal hamstring complex remains controversial. A complete tear is characterized by complete disruption of the involved tendinous or aponeurotic structure, which may or may not be associated with retraction of the disrupted tendon ends. Surgical repair is commonly considered in high-level athletes with complete tears, particularly in cases of two-tendon avulsions with more than 2 cm of retraction and complete three-tendon avulsions, although exact indications remain debated [9–18].

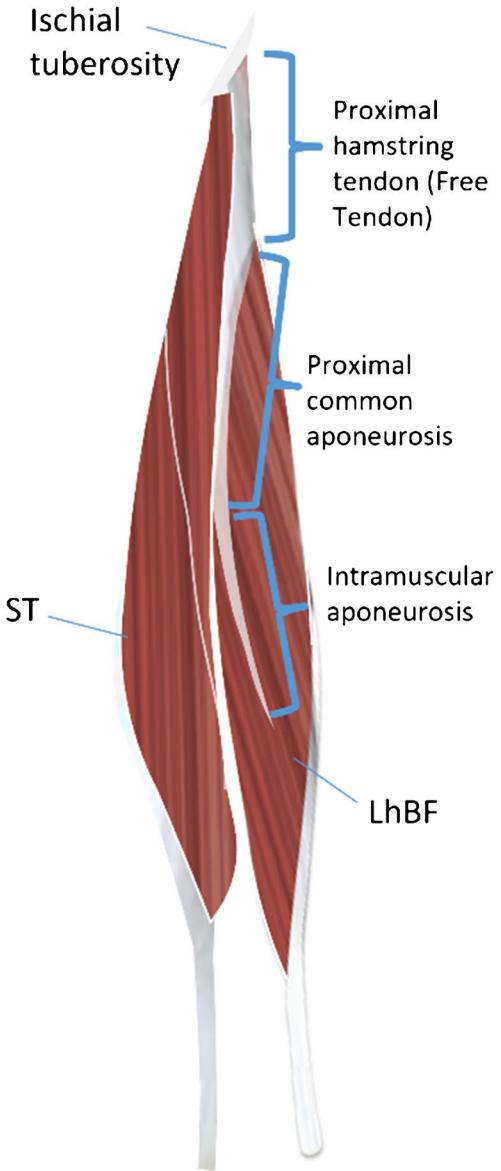


Fig. 1 Schematic illustration of the proximal hamstring musculotendinous complex, showing the free tendon, proximal common aponeurosis, and intramuscular aponeurosis of the long head of biceps femoris (LhBF). Semitendinosus (ST)

Postoperative recovery is monitored through clinical assessment, load progression, strength testing, and GPS data, with magnetic resonance imaging (MRI) playing an increasingly important complementary role [19, 20]. MRI is considered the gold standard for diagnosing hamstring injuries and is widely used to track the healing process in elite athletes [21–23]. Recent studies have characterized the MRI appearance of conservatively managed myoconnective injuries [21, 22] and identified MRI signs associated with reinjury risk prior to return to play [24]. However,

postoperative tendon healing follows a different biological process and therefore demonstrates MRI findings that differ from those observed after conservative treatment.

To our knowledge, no study has comprehensively characterized the MRI appearance of uncomplicated postoperative tendon healing after proximal hamstring repair. The aim of this study was to characterize the temporal MRI appearance of uncomplicated healing during the first 4 months following surgical repair of proximal hamstring musculotendinous complex tears.

Materials and methods

A consecutive case series (Level of Evidence IV) was conducted at a single professional football club and included professional football players with MRI-confirmed complete tears of the proximal hamstring musculotendinous complex who underwent surgical repair between May 2017 and December 2025. The study was approved by the club's Local Ethics Committee and Sports Medical Department. Consecutive patients undergoing surgical repair underwent postoperative MRI follow-up as part of routine clinical practice. For the present study, medical records, surgical reports, and MRI examinations were retrospectively reviewed to confirm the diagnosis, surgical treatment, and availability of postoperative MRI follow-up. For the purposes of this study, a complete tear of the proximal hamstring musculotendinous complex was defined as complete disruption of the proximal free tendon, proximal common aponeurosis, or junction between these two structures within the long head of the biceps femoris–semitendinosus complex, without requiring avulsion from the ischial tuberosity.

Inclusion criteria were MRI-confirmed acute complete tears of the proximal hamstring musculotendinous complex treated surgically using the same operative approach and consent to undergo serial postoperative MRI examinations. Patients who declined MRI follow-up or had insufficient image quality were excluded. Patients with an uncomplicated postoperative course were included in the primary descriptive cohort, whereas those who developed a postoperative exacerbation during the healing period were excluded from this cohort and reviewed separately in an exploratory descriptive analysis. An exacerbation was defined as worsening of a non-recovered index injury, according to the framework proposed by Finch and Cook [25]. The exploratory descriptive analysis was intended to document the MRI findings observed before the exacerbation, rather than to compare imaging outcomes between groups or identify imaging predictors of exacerbation. No a priori sample-size calculation was performed; the study sample comprised all consecutive eligible cases identified during the study period.

The surgical procedure was undertaken using the technique described by Orava and Lempainen [26]. It consisted of a vertical incision over the injured area, fasciotomy, identification of the ruptured tendon, and tendon repair. Tears located within 8–12 cm distal to the ischial tuberosity were repaired using a single suture anchor inserted into the ischial tuberosity for reinforcement. More distal tendon tears were repaired by approximating the tendon ends and incorporating the adjacent semitendinosus and biceps femoris muscle tissue into the repair, without inserting a suture anchor into the bone.

All postoperative MRI examinations were performed using an MRI scanner located at the club's training facilities. Postoperative MRI examinations were available for 22 of the 24 surgically repaired tendons, as two patients declined postoperative MRI follow-up. Of these 22 tendons, 7 were scanned with a Vantage Titan 3 T (Canon, Shimomaruko, Tokyo, Japan), and 15 tendons with a Vantage Galan 3 T (Canon, Shimomaruko, Tokyo, Japan). The follow-up MRI protocol consisted of three sequences: two fluid-sensitive sequences (axial and coronal), acquired as T2-weighted fat-suppressed (T2-FS) or proton density fat-suppressed (PD-FS), and one axial T1-weighted sequence. Imaging parameters on the Vantage Titan system were as follows: axial T2-FS (TR/TE, 5200/44 ms; slice thickness, 3.5 mm; FOV, 25 × 25 cm), coronal T2-FS (TR/TE, 5000/44 ms; slice thickness, 2.5 mm; gap, 0.6 mm; FOV, 26 × 29 cm), and axial T1-weighted imaging (TR/TE, 900/11 ms; slice thickness, 3.5 mm; FOV, 25 × 25 cm). Imaging parameters on the Vantage Galan system were as follows: axial PD-FS (TR/TE, 2900/33 ms; slice thickness, 3.5 mm; FOV, 23 × 23 cm), coronal PD-FS (TR/TE, 2700/44 ms; slice thickness, 2.5 mm; gap, 0.4 mm; FOV, 25 × 25 cm), and axial T1-weighted imaging (TR/TE, 740/10 ms; slice thickness, 3.5 mm; FOV, 22 × 22 cm). The examination time was approximately 15 min. Patients were examined in the supine position using a combination of Atlas SPEEDER body and spine coils. The feet were secured in a neutral position with a strap to ensure consistent lower-limb positioning across all serial examinations.

MRI studies were independently reviewed by two musculoskeletal radiologists with 3 and 12 years of experience. Before image analysis, both readers underwent a 1-month training period to standardize the interpretation criteria for each MRI finding. Each reader independently evaluated the serial MRI examinations from the same patient. Acquisition dates were visible, allowing the readers to recognize the chronological order of the examinations; however, they were blinded to the time elapsed since surgery and were therefore unaware of the specific postoperative month corresponding to each examination. The readers were also blinded to patient identity, clinical information, and rehabilitation

outcome. This blinding was intended to minimize potential observer bias during MRI assessment. Disagreements were resolved by consensus, with adjudication by a third musculoskeletal radiologist with 16 years of experience when required. Interobserver agreement between the two readers was assessed using Cohen's kappa statistic (weighted kappa for scar maturation) before consensus review. For features with markedly unbalanced category distributions resulting in potentially misleading or non-informative κ estimates, Gwet's first-order agreement coefficient (AC1) with 95% confidence intervals was additionally calculated as a complementary measure of interobserver agreement.

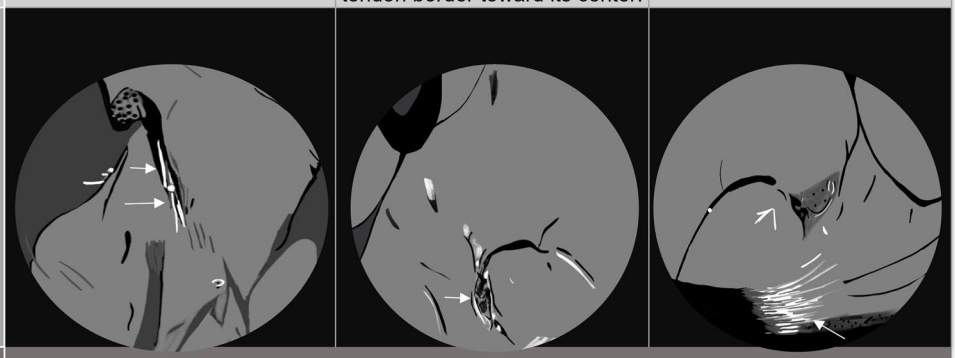
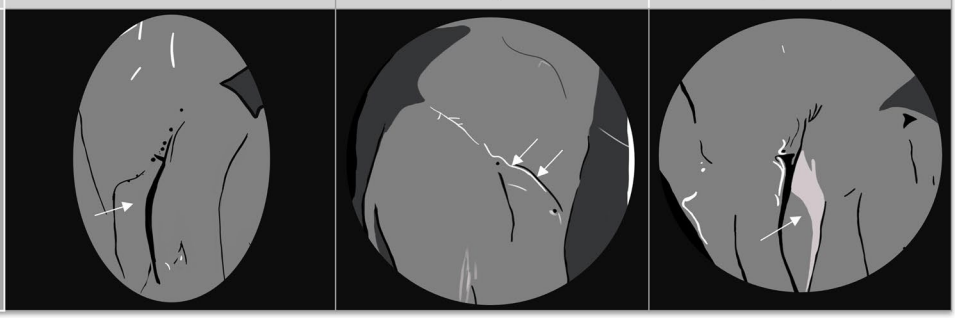
Eight MRI features of postoperative tendon healing were assessed: longitudinal intratendinous clefts, transverse intratendinous clefts, scar maturation [21, 22], edema-like signal (interstitial, intermuscular, or adaptive), postoperative subcutaneous soft-tissue signal change, tendinous angulation, blunt muscle outline, and denervation-like signal. Longitudinal intratendinous clefts (LIC) were defined as fluid-sensitive linear hyperintense clefts oriented predominantly parallel to the longitudinal axis of the repaired tendon, whereas transverse intratendinous clefts (TIC) were defined as fluid-sensitive linear hyperintense clefts oriented predominantly perpendicular to the longitudinal axis of the tendon, extending from the tendon border toward its center. Classification was based on the orientation of the cleft relative to the tendon rather than on the imaging plane in which it was visualized. LIC and TIC were recorded as present or absent at each examination. During serial review, interval changes in the extent and signal intensity of LIC, TIC, and edema-like signal were also assessed qualitatively by comparison with the preceding examination; however, these changes were not quantitatively measured or graded using a predefined scale. Scar maturation was assessed as a binary variable and classified as immature (healing phases 1 and 2, the latter comprising subphases 2A and 2B) or mature (healing phase 3, comprising subphases 3A and 3B, and the final healed stage [FHS]) according to the MRI healing classification previously described by Isern-Kebschull et al. [21]. An immature scar was defined as a scar with a hyperintense central component on PD-FS images, whereas a mature scar was characterized by a predominantly hypointense center on PD-FS images and a well-organized tendon architecture on PD-FS and T1-weighted images. Edema-like signal was categorized according to its distribution as interstitial, intermuscular, or adaptive. On PD-FS images, interstitial edema-like signal was defined as a feathery hyperintense pattern within the interstitial space between muscle fibers; intermuscular edema-like signal as a laminar hyperintense pattern along the intermuscular or perifascial planes; and adaptive edema-like signal as mild, ill-defined hyperintense signal surrounding a mature scar [22]. Postoperative subcutaneous soft-tissue signal change was defined as abnormal signal within the subcutaneous tissues adjacent to the surgical approach, including early postoperative fluid/hemorrhagic-appearing signal and persistent postoperative signal alteration during subsequent follow-up. Tendinous angulation was defined as an abnormal focal change in the expected longitudinal course of the repaired tendon, resulting in a visible angular deformity rather than a smooth linear trajectory. Blunt muscle outline was defined as loss of the normal tapered contour of the proximal muscle belly, resulting in a rounded or truncated appearance at its proximal end. Denervation-like signal was defined as intramuscular hyperintense signal abnormality on fluid-sensitive sequences with a geographic distribution within the semitendinosus and/or long head of the biceps femoris that did not correspond to the extent of the surgical repair. The signal abnormality could be relatively well demarcated and was not associated with fascial or subcutaneous edema-like signal [27]. Fatty infiltration was not used as a criterion for denervation-like signal. Operational definitions and schematic illustrations of all evaluated MRI features are provided in Table 1 and Fig. 2.

Postoperative exacerbations during rehabilitation, subsequent hamstring injuries, and postoperative symptoms suggestive of sciatica were prospectively recorded. Players were subsequently monitored clinically for up to 2 years while they remained at the club to identify muscle injuries potentially related to the previous surgical repair and the development of postoperative sciatic symptoms.

Data analysis

The statistical analysis was primarily descriptive. All variables analyzed were categorical and are reported as absolute frequencies and percentages. Because postoperative MRI examinations were not available for every tendon at each monthly time point, monthly frequencies were treated as cross-sectional descriptive data. Temporal changes in the principal MRI findings were additionally assessed within individual tendons with at least two postoperative MRI examinations by comparing the first and last available examinations. This longitudinal descriptive analysis evaluated resolution of longitudinal and transverse intratendinous clefts, progression from an immature to a mature scar, and resolution of edema-like signal. It also assessed the persistence of tendinous angulation, blunt muscle outline, and evolution of postoperative subcutaneous soft-tissue signal change, as well as the development of denervation-like signal. For this analysis, edema-like signal was considered present when interstitial and/or intermuscular edema-like signal was identified. Tendons with only one postoperative MRI examination contributed to the monthly descriptive analysis

Table 1 Characteristic MRI features of uncomplicated postoperative healing after surgical repair of proximal hamstring tendon injuries: definitions and schematic illustrations

MRI FEATURE	LONGITUDINAL INTRATENDINOUS CLEFTS	TRANSVERSE INTRATENDINOUS CLEFTS	POSTOPERATIVE SUBCUTANEOUS SOFT-TISSUE SIGNAL CHANGE
DESCRIPTION	Linear intratendinous hyperintense clefts oriented along the longitudinal axis of the tendon.	Presence of intratendinous hyperintense clefts visible in the axial plane, extending from the tendon border toward its center.	Abnormal signal within the subcutaneous tissues adjacent to the surgical approach.
ILLUSTRATION			
MRI FEATURE	TENDINOUS ANGULATION	BLUNT OUTLINE	DENERVATION-LIKE SIGNAL
DESCRIPTION	Angular deviation of the repaired tendon from its expected anatomical course.	Loss of the normal tapered contour of the proximal long head of the biceps femoris muscle belly, resulting in a rounded appearance.	Geographic intramuscular hyperintensity on fluid-sensitive images, with a distribution unrelated to the extent of the surgical repair.
ILLUSTRATION			

but were not included in the within-tendon longitudinal analysis. The final follow-up MRI was defined as the last available postoperative MRI examination for each individual tendon. Because some players contributed bilateral injuries and individual tendons underwent repeated MRI examinations, observations were not considered statistically independent. Accordingly, no inferential analyses treating individual MRI examinations or tendons as independent observations were performed.

Artificial intelligence–assisted language editing

During manuscript preparation and revision, ChatGPT (OpenAI) was used to assist with English-language editing and to improve the clarity and readability of the text. The tool was not used for data collection, image interpretation, statistical analysis, or generation of scientific results. All AI-assisted text was critically reviewed and edited by the authors, who take full responsibility for the final content of the manuscript.

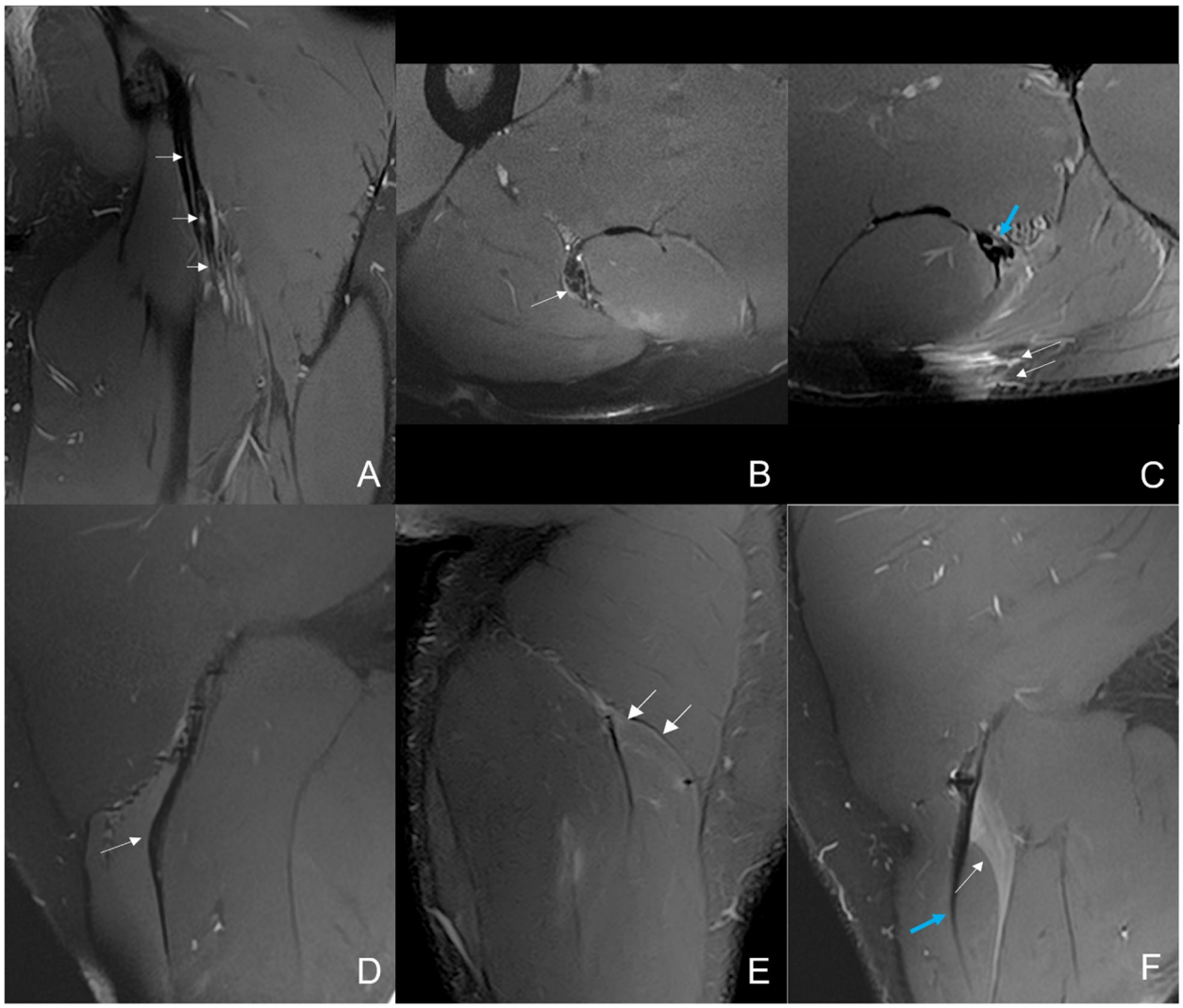


Fig. 2 Coronal and axial proton density fat-suppressed MR images illustrating characteristic MRI findings following surgical repair of complete tears of the proximal hamstring complex in different patients. **A** Longitudinal intratendinous clefts (arrows) at the second postoperative follow-up. **B** Transverse intratendinous clefts (arrow) at the second postoperative follow-up, extending from the tendon periphery toward its center. **C** Persistent postoperative subcutaneous soft-tissue signal change (arrows) at the third postoperative follow-up, with a residual transverse intratendinous cleft (TIC). Clinical pearl: Residual intratendinous clefts (blue arrow) may persist during the remodeling phase and do not necessarily indicate failed healing. **D** Persistent tendinous angulation (arrow) at the fourth postoperative follow-up. **E** Blunt outline of the long head of the biceps femoris muscle belly (arrows) at the third postoperative follow-up. **F** Prominent denervation-like signal (arrow) within the semitendinosus muscle at the fourth postoperative follow-up, with persistent tendinous angulation. Clinical pearl: Tendinous angulation (blue arrow) may persist during uncomplicated healing and, in isolation, should not be interpreted as evidence of failed healing

Results

Study population

Twenty male professional football players aged 16 to 25 years (mean age ± SD, 19 ± 1.4 years) met the inclusion criteria. Four players sustained bilateral injuries during different seasons, resulting in a total of 24 complete tears of the proximal hamstring musculotendinous complex. The tears involved the free tendon in 15 cases, the proximal common aponeurosis in five, and the junction between the free tendon and the proximal common aponeurosis in four. None of the 24 injuries included in the study showed associated semimembranosus tendon involvement on the initial diagnostic MRI. Diagnostic MRI was performed within 24–48 h after injury in all cases, and surgical repair was undertaken at a mean of 8 days after injury (range, 3–16 days). Fourteen tendons were repaired

by one surgeon and ten by a second surgeon. Among the 24 surgically repaired tendons, a single-anchor reinforcement was used in 11 cases and direct tendon repair without anchor fixation in 13. Among the 15 tendons included in the primary descriptive cohort, 7 underwent single-anchor reinforcement and 8 underwent direct tendon repair. No consistent differences in the evaluated postoperative MRI healing features were observed between tendons repaired with anchor reinforcement and those repaired without anchor fixation.

Fifteen tendons constituted the primary descriptive cohort of uncomplicated postoperative healing. Two patients declined postoperative MRI follow-up, one patient was excluded after sustaining an anterior cruciate ligament rupture during rehabilitation, and six tendons were excluded from the primary descriptive cohort because of postoperative exacerbations and were reviewed separately in an exploratory descriptive analysis (Fig. 3).

All tendons in both the uncomplicated-healing cohort and the exploratory exacerbation subgroup were classified as grade 4c according to the BAMIC [28] and as IPp3^{r} according to the MLG-R classification [29]. According to the MRI-based classification proposed by Forlizzi et al. [18], all injuries corresponded to Type 2c, representing isolated complete tears of the conjoint tendon (LhBF–ST complex) without semimembranosus involvement. In the uncomplicated-healing cohort, the injury involved the free tendon in 9/15 (60.0%), the proximal common aponeurosis in 5/15 (33.3%), and the junction between the free tendon and proximal common aponeurosis in 1/15 (6.7%). No consistent differences in the evaluated postoperative MRI healing features were observed according to the anatomical location of the index tear (free tendon, proximal common aponeurosis, or junction between these structures). Among the six tendons that subsequently developed an exacerbation, 4/6 (66.7%) involved the free tendon and 2/6 (33.3%) the junction. Single-anchor reinforcement was used in 7/15 (46.7%) tendons in the uncomplicated-healing cohort and in 2/6 (33.3%) tendons in the exploratory exacerbation subgroup. Given the small number of exacerbation cases and the exploratory nature of this subgroup, no inferential between-group comparisons were performed.

MRI follow-up

During holiday periods and international call-ups, players were often away from the club. In addition, postoperative MRI follow-up depended on both the surgeon's protocol and the club's medical requirements. Consequently, it was not possible to obtain monthly MRI examinations in all cases. A total of 43 postoperative MRI examinations were analyzed: 12 during the first postoperative month, 10 during the second month, 14 during the third month, and 7 during the fourth month. The distribution of postoperative MRI follow-up examinations is summarized in Supplementary Table S1.

Interobserver agreement for the evaluated MRI findings is presented in Table 2. Agreement was almost perfect for scar maturation (weighted $\kappa = 0.922$; 95% CI, 0.84–1.00), substantial for LIC ($\kappa = 0.621$; 95% CI, 0.39–0.85) and denervation-like signal ($\kappa = 0.771$; 95% CI, 0.59–0.95), moderate

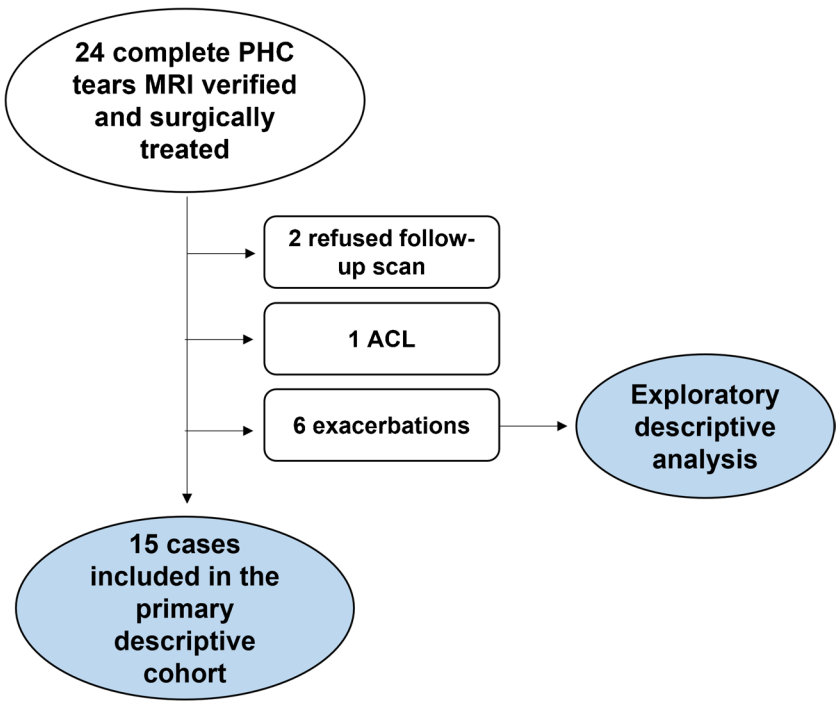


Fig. 3 Flowchart of the participants in the study. PHC, proximal hamstring complex

Table 2 Interobserver agreement for postoperative MRI findings

MRI feature	Agreement	Cohen's κ	95% CI	Gwet's AC1 (95% CI)
LIC	81.4%	0.621	0.39–0.85	-
TIC	81.4%	0.580	0.33–0.83	-
Scar maturation*	86%	0.922	0.84–1	-
Intermuscular edema-like signal	95.3%	0.878	0.71-1	-
Interstitial edema-like signal	90.7%	0.801	0.62-0.99	-
Adaptive edema-like signal	95.3%	NE	NE	0.951 (0.88-1)
Postoperative subcutaneous soft-tissue signal change	100%	1	1–1	-
Tendinous angulation	69.8%	−0.167	−0.27 to −0.065	0.593 (0.349-0.837)
Blunt outline	79.1%	0.396	0.076–0.72	-
Denervation-like signal	88.4%	0.771	0.59–0.95	-

*Weighted Cohen's κ using quadratic weights

Gwet's AC1 was additionally calculated for features with markedly unbalanced category distributions for which Cohen's κ was potentially misleading or non-informative. For adaptive edema-like signal, one reader classified all examinations as positive, precluding a meaningful estimation of Cohen's κ. *CI* confidence interval, *LIC* longitudinal intratendinous cleft, *TIC* transverse intratendinous cleft, *NE* not estimable

for TIC ($\kappa = 0.580$; 95% CI, 0.33–0.83), and fair for blunt muscle outline ($\kappa = 0.396$; 95% CI, 0.076–0.72). Intermuscular and interstitial edema-like signal showed almost perfect agreement ($\kappa = 0.878$; 95% CI, 0.71–1.00) and substantial agreement ($\kappa = 0.801$; 95% CI, 0.62–0.99), respectively. Postoperative subcutaneous soft-tissue signal change showed perfect agreement ($\kappa = 1.000$; 95% CI, 1.00–1.00). For tendinous angulation, observed agreement was 69.8%, whereas Cohen's κ was −0.167 (95% CI, −0.27 to −0.065). Given the markedly unbalanced category distribution, Gwet's AC1 was additionally calculated and was 0.593. For adaptive edema-like signal, observed agreement was 95.3%; because one reader classified all examinations as positive, Cohen's κ was not informative, whereas Gwet's AC1 was 0.951.

Uncomplicated postoperative MRI evolution

LIC were observed in 11 of 15 cases (73.3%), TIC in 13 of 15 (86.7%), postoperative subcutaneous soft-tissue signal change in all 15 cases (100%), tendinous angulation in all 15 cases (100%), a blunt outline of the muscle belly in 13 of 15 cases (86.7%), and denervation-like signal in 10 of 15 cases (66.7%). The denervation-like signal involved the semitendinosus (ST) alone in seven cases, the LhBF alone in two cases, and both muscles in one case.

All evaluated MRI findings were observed from the first postoperative month except denervation-like signal, which was first observed during the second postoperative month. Thirteen of the 15 tendons had at least two postoperative MRI examinations and were included in the within-tendon longitudinal descriptive analysis. LIC and TIC resolved by the last available MRI in 6/10 (60%) and 7/12 (58.3%) tendons in which they were initially present, respectively. Residual clefts persisted in a substantial proportion of tendons, consistent with ongoing tendon remodeling [30–32]. On qualitative serial assessment, edema-like signal generally decreased in extent and intensity, while a more adaptive pattern was observed during later follow-up [33]. In contrast, postoperative subcutaneous soft-tissue signal change persisted in most cases until the final follow-up. Likewise, tendinous angulation and a blunt outline of the muscle belly, when present on the initial postoperative MRI, remained visible at the last follow-up examination. During the second postoperative month, 9/10 (90%) tendons demonstrated a mature scar (phases 3A–3B). Among the seven MRI examinations performed during the fourth postoperative month, all tendons exhibited a mature scar: four (57.1%) were in phase 3 A, two (28.6%) in phase 3B, and one (14.3%) in the FHS. The cross-sectional distribution of MRI findings according to postoperative month is shown in Table 3. Because not all tendons were examined at every monthly time point, these frequencies represent the MRI examinations available within each postoperative month and should not be interpreted as within-tendon rates of resolution or progression.

Within-tendon temporal evolution of the primary MRI findings is shown in Table 4. Among the 10 tendons with

Table 3 Distribution of MRI findings by postoperative month

	FIRST MONTH (12 cases)	SECOND MONTH (10 cases)	THIRD MONTH (14 cases)	FOURTH MONTH (7 cases)
MRI SIGNS	LIC (10, 83.3%) TIC (11, 91.7%) Immature healing stage (11, 91.7%) All type edemas (12, 100%) Postoperative subcutaneous soft-tissue signal change (12, 100%) Tendinous angulation (12, 100%) Blunt outline (10, 83.3%)	LIC (7, 70%) TIC (7, 70%) Mature healing stage (9, 90%) Interstitial and intermuscular edemas (9, 90%) Adaptive edema (10, 100%) Postoperative subcutaneous soft-tissue signal change (10, 100%) Tendinous angulation (9, 90%) Blunt outline (9, 90%) Denervation (7, 70%)	LIC (5, 35.7%) TIC (8, 57.1%) Mature healing stage (14, 100%) Interstitial edema (10, 71.4%) Adaptive edema (13, 92.8%) Postoperative subcutaneous soft-tissue signal change (13, 92.8%) Tendinous angulation (13, 92.8%) Blunt outline (11, 78.6%) Denervation (10, 71.4%)	LIC (2, 28.6%) TIC (2, 28.6%) Mature healing stage (7, 100%) Adaptive edema (7, 100%) Interstitial edema (1, 14.3%) Postoperative subcutaneous soft-tissue signal change (7, 100%) Angulation (6, 85.7%) Blunt outline (5, 85.7%) Denervation (6, 71.4%)

LIC longitudinal intratendinous clefts, *TIC* transverse intratendinous clefts

LIC on their first available MRI, LIC resolved by the last available MRI in 6/10 (60.0%) and persisted in 4/10 (40.0%). TIC resolved in 7/12 (58.3%) tendons in which it was present on the first available MRI and persisted in 5/12 (41.7%). Although residual LIC and TIC persisted in some tendons at the last available MRI, qualitative serial assessment showed a reduction in their extent and signal intensity. All 10/10 (100%) tendons with an immature scar (phase 2 A or 2B) on their first available MRI progressed to a mature scar (phase 3 and final healed stage [FHS]) by the last available examination. Edema-like signal resolved in 7/13 (53.8%) tendons and persisted in 6/13 (46.2%). Among the 12 tendons without denervation-like signal on their first available MRI, 9/12 (75.0%) developed this finding during subsequent follow-up.

Table 4 Within-tendon temporal evolution of the primary postoperative MRI findings

TENDON	MRI FOLLOW-UP	LIC	TIC	SCAR PHASE	EDEMA-LIKE SIGNAL	DENERVATION-LIKE SIGNAL
1	F3	-	-	3A	+	-
2	F1-F2-F3-F4	+→+→-→-	+→+→-→-	2A→3A→3A→FHS	+→+→+→-	-→+→+→+
3	F3-F4	-→-	+→-	3B→3B	+→-	+→+
5	F1-F2-F3	-→-→-	-→-→-	3A→3A→3B	+→+→+	-→-→-
6	F1-F2-F3	+→+→+	+→+→+	2A→3A→3A	+→+→-	-→+→+
7	F1-F2-F3	-→-→-	+→-→-	2B→3A→3B	+→+→+	-→+→+
8	F1-F3-F4	+→+→-	+→+→-	2A→3A→3A	+→-→-	-→+→+
9	F2-F3	+→-	+→-	3A→3A	+→+	-→-
12	F1-F2-F3	+→+→-	+→+→+	2A→2B→3A	+→+→-	-→+→+
16	F1-F2-F3-F4	+→-→-→-	+→-→-→-	2A→3A→3A→3B	+→+→+→+	-→+→+→+
18	F1-F3-F4	+→+→+	+→+→+	2A→3A→3A	+→+→+	-→+→+
19	F1-F2-F3	+→+→+	+→+→+	2B→3A→3A	+→+→-	-→+→+
20	F1-F2-F3-F4	+→+→-→-	+→+→+→-	2A→3A→3A→3A	+→+→+→+	+→+→+→+
21	F1-F2-F3-F4	+→+→+→+	+→+→+→+	2A→3A→3A→3A	+→+→+→+	-→-→-→-
22	F1	+	+	2B	+	-

F1–F4 indicate postoperative months 1–4, respectively. +, presence; −, absence; *LIC* longitudinal intratendinous cleft, *TIC* transverse intratendinous cleft, *FHS* final healed stage. Edema-like signal was considered present when interstitial and/or intermuscular edema-like signal was identified

Figure 4 illustrates the sequential MRI appearance of a surgically repaired proximal hamstring tendon over the first four postoperative months.

MRI findings preceding postoperative exacerbation

Six tendons that developed postoperative exacerbations during rehabilitation were excluded from the primary descriptive cohort of uncomplicated postoperative healing and were reviewed separately. Three exacerbations occurred during the fourth postoperative month, two during the third month, and one during the fifth month. In four of the six tendons, the MRI examination immediately preceding exacerbation demonstrated extensive, prominent longitudinal and transverse intratendinous clefts that were markedly hyperintense on PD-FS images, together with an immature scar, an intratendinous cavity, or persistent interstitial edema-like signal. The clinical characteristics and descriptive MRI findings of these six tendons are summarized in Supplementary Table S2.

Subsequent hamstring injuries

Five subsequent hamstring injuries occurred during follow-up. Four involved the LhBF distal to the repaired tendon (10–18 months after surgery), whereas one involved the semitendinosus during the fourth postoperative month. All five injuries presented as new clinical injury events and were subsequently confirmed by diagnostic MRI performed specifically to evaluate the new injury; they were not identified on routine postoperative follow-up MRI.

Discussion

The present study provides a detailed description of the MRI appearance of postoperative healing following surgical repair of complete tears of the proximal hamstring musculotendinous complex. Surgical repair is considered in selected patients with complete proximal hamstring musculotendinous complex tears, particularly high-level athletes, although the optimal indications remain debated [9, 10]. To our knowledge, this is the first study to systematically characterize the temporal evolution of specific MRI findings during the first four postoperative months. Characterizing the postoperative MRI appearance is important because persistent structural abnormalities may be observed during otherwise uncomplicated healing and should be interpreted within the context of postoperative tendon remodeling.

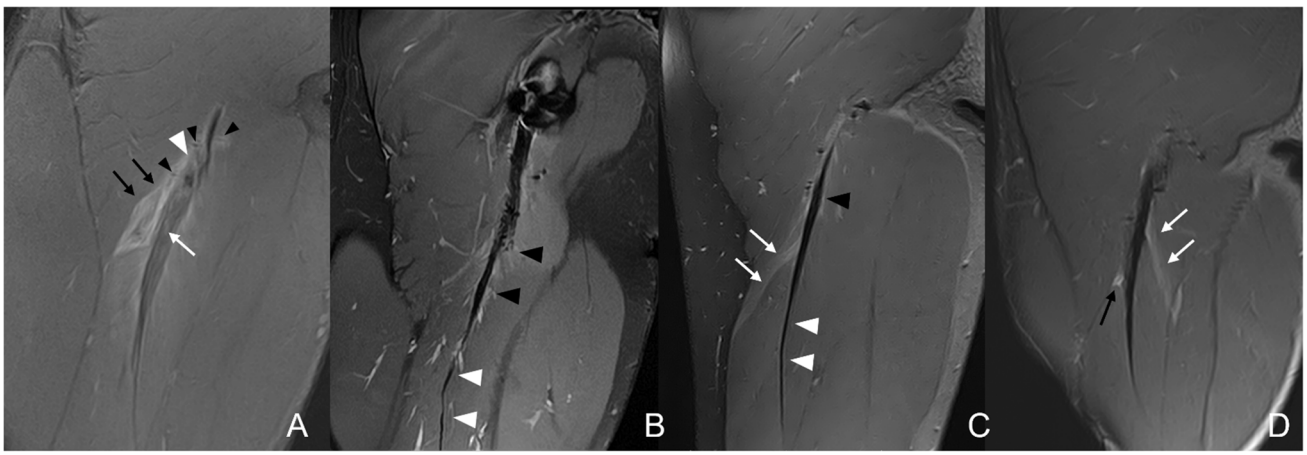


Fig. 4 Coronal proton density fat-suppressed MR images from the same patient illustrating the sequential healing process following surgical repair of a complete tear of the proximal hamstring musculotendinous complex. Images were selected at closely comparable, although not identical, anatomical levels to best demonstrate the evolution of the postoperative findings. **A** First postoperative month. The repair site demonstrates longitudinal intratendinous clefts (white arrow), an immature scar (white arrowhead), and a blunt outline of the long head of the biceps femoris (LhBF) muscle belly (black arrows). Susceptibility artifact from the surgical suture is visible adjacent to the repair site (black arrowheads). **B** Second postoperative month. The repaired tendon appears more organized, with a mature scar and mild tendinous angulation (white arrowheads). Small foci of interstitial edema are also present (black arrowhead). **C** Third postoperative month. The repaired tendon shows a more organized appearance. A band of edema-like signal is present within the LhBF (arrows), suggestive of denervation. Small foci of interstitial edema (black arrowheads) and persistent tendinous angulation (white arrowheads) are also present. **D** Fourth postoperative month. The repaired tendon demonstrates a mature postoperative appearance. A denervation-like band is present within the semitendinosus muscle (white arrows), while a blunt outline of the LhBF muscle belly persists (black arrow). This temporal evolution illustrates that scar maturation and structural normalization do not necessarily occur simultaneously; residual postoperative abnormalities may persist despite progressive scar maturation

Eight MRI findings were evaluated to characterize the postoperative healing process. In our surgically treated cases, the ruptured tendon fibers were retracted and frayed. Their reapproximation during surgical repair may explain the longitudinal and transverse intratendinous clefts observed on postoperative MRI. Similar postoperative intratendinous hyperintense areas have been described after Achilles tendon repair, where they are considered part of the normal tendon remodeling process rather than evidence of failed healing [34]. These similarities suggest that residual intratendinous clefts following proximal hamstring tendon repair may represent part of the structural remodeling process rather than necessarily indicating incomplete healing.

Scar maturation should also be interpreted within the context of postoperative tendon remodeling. At the final follow-up examination, a tendon may demonstrate a mature scar while still showing residual intratendinous signal heterogeneity (phase 3 A), reflecting ongoing remodeling rather than incomplete healing. Importantly, intratendinous clefts and scar maturation represent different aspects of the healing process. Whereas scar maturation reflects the biological evolution of the reparative tissue, intratendinous clefts reflect the structural organization of the repaired tendon. Consequently, a tendon may demonstrate a mature scar while still exhibiting residual clefts during the remodeling phase.

Tendinous angulation was observed in all tendons in the primary descriptive cohort and may represent a morphological consequence of tendon retraction and subsequent surgical reapproximation. Following rupture, tendon retraction alters the normal longitudinal configuration of the musculotendinous complex; surgical repair restores tendon continuity and tension but may leave a persistent angulated configuration. Similarly, the blunt outline of the proximal LhBF muscle belly may result from the altered orientation and pennation of the proximal muscle fibers following tendon rupture and retraction, rather than representing incomplete healing. Similar morphological changes can occasionally be observed after conservatively treated proximal myotendinous injuries of the LhBF without apparent functional impairment [21, 24, 35]. Therefore, these postoperative morphological abnormalities should not be considered synonymous with failed tendon healing.

The denervation-like signal was the only MRI finding that was not observed during the first postoperative month, becoming apparent from the second postoperative month. This temporal pattern is consistent with the observations of Gutmann et al. and Fleckenstein et al., who reported that MRI is relatively insensitive during the first weeks following complete nerve disruption, paralleling the well-recognized low sensitivity of electromyography during the same period [36, 37]. Although electrophysiological studies were not performed, the distribution of the denervation-like signal is possibly due to involvement of small sciatic nerve branches during surgical dissection. The semitendinosus was the most frequently affected muscle. Similar signal abnormalities have been reported during postoperative follow-up by Sgustav et al. [19]. Whether the denervation-like signal observed in our cohort represents a transient postoperative change requires further longitudinal evaluation.

Lin et al. [38] reported postoperative sciatica in older patients undergoing delayed surgical repair, with MRI demonstrating sciatic nerve tethering, extensive perineural scarring, and persistent denervation edema. In contrast, our cohort consisted of young athletes treated at a mean of 8 days after injury, and no patient developed clinical postoperative sciatica during follow-up. Whether differences in surgical timing contributed to the absence of postoperative sciatica in our cohort remains uncertain and requires further investigation.

The within-tendon descriptive longitudinal analysis revealed different temporal patterns among the evaluated postoperative MRI findings. LIC and TIC resolved in more than half of the tendons in which they were initially present. Although residual clefts persisted in a substantial proportion of tendons at the last available MRI, qualitative serial assessment showed a reduction in their extent and signal intensity. In contrast, scar maturation showed a more consistent temporal evolution, with all tendons demonstrating an immature scar on their first available MRI progressing to a mature scar by final follow-up. Edema-like signal resolved in approximately half of the tendons, whereas denervation-like signal frequently developed during follow-up. Other structural abnormalities, including tendinous angulation and blunt muscle outline, frequently persisted. Taken together, these findings indicate that postoperative tendon healing is not characterized by the simultaneous resolution of all MRI abnormalities. Instead, scar maturation may coexist with persistent structural and signal abnormalities, highlighting the importance of interpreting individual MRI findings within the broader context of postoperative tendon remodeling.

Six tendons that developed postoperative exacerbations were not included in the primary descriptive cohort of uncomplicated healing and were reviewed separately. On the MRI examination immediately preceding exacerbation, the intratendinous clefts in four of the six tendons remained extensive and showed marked hyperintensity on PD-FS images, with a prominent appearance, suggesting less advanced structural remodeling at the time of imaging. Other findings included an immature scar, an intratendinous cavity, and persistent interstitial edema-like signal. However, because this was a small exploratory subgroup defined by subsequent clinical outcome, these observations should not be interpreted as imaging predictors of postoperative

exacerbation or as evidence of differences between uncomplicated and complicated healing. Rather, they should be considered hypothesis-generating observations that require validation in larger prospective cohorts including both uncomplicated and adverse postoperative outcomes.

Five subsequent hamstring injuries occurred during follow-up. Interestingly, most subsequent injuries did not occur at the repaired tendon itself but at a distal location within the same musculotendinous unit. One possible explanation is that restoration of tendon tension after surgical repair may modify force transmission within the musculotendinous unit, potentially contributing to biologically related injuries at a different anatomical location. Although these events cannot be interpreted as true recurrences, they may represent biologically related injuries reflecting persistent alterations in force transmission, tissue adaptation, or load distribution following the index injury. This interpretation remains speculative and requires confirmation in prospective studies.

The optimal frequency and duration of MRI surveillance after proximal hamstring repair remain uncertain. In the present study, the focus on the first four postoperative months reflected the minimum time-loss period before return to play in our cohort, rather than an established imaging surveillance interval. Epidemiological data from professional football indicate that approximately 18% of hamstring injuries are recurrences and that more than two-thirds occur within 2 months after return to play [3]; however, these data are not specific to surgically repaired proximal hamstring injuries. Therefore, the present findings do not support a standardized postoperative MRI schedule, and imaging follow-up should be individualized according to clinical and rehabilitation progression.

Interobserver agreement varied across the evaluated MRI features. Scar maturation, LIC, denervation-like signal, and intermuscular and interstitial edema-like signal showed generally high interobserver agreement, whereas agreement was lower for TIC and blunt muscle outline, suggesting greater reader dependence for these descriptors. The lower agreement for TIC may partly reflect the three-dimensional orientation of intratendinous clefts: a LIC may appear transverse on an axial image, and confirmation of a true TIC therefore requires assessment of its extension and orientation along the tendon axis across imaging planes. Assessment of blunt muscle outline may also be more challenging because the contour of the proximal muscle belly can be partially obscured by the overlying gluteus maximus, potentially contributing to reader variability. For tendinous angulation and adaptive edema-like signal, Cohen's κ was affected by markedly unbalanced category distributions and therefore did not adequately reflect the observed agreement. For tendinous angulation, complementary analysis using Gwet's AC1 indicated a substantially higher level of agreement than suggested by κ, although agreement remained lower than for most other evaluated features. Assessment of tendinous angulation may be influenced by technical factors. Because relatively small fields of view were used, the midportion of the proximal myotendinous junction could occasionally lie near the periphery of the image, where geometric distortion may alter the apparent course of the tendon and potentially contribute to reader disagreement. For adaptive edema-like signal, the very high observed agreement was supported by Gwet's AC1, indicating high interobserver reproducibility despite the inability of Cohen's κ to provide an informative estimate.

This study has several limitations. First, the logistics of a professional football club made it difficult to obtain standardized monthly MRI examinations in every player, which may have influenced the reported prevalence of some imaging findings. Second, the sample size was relatively small, particularly for postoperative exacerbations, precluding inferential analysis of adverse healing outcomes. Third, the primary descriptive cohort was defined retrospectively according to an uncomplicated postoperative course, with exclusion of tendons that subsequently developed exacerbations, introducing potential outcome-based selection bias. Therefore, the MRI findings described in this cohort should be interpreted as the imaging evolution observed in uncomplicated postoperative healing rather than as a reference standard for normal healing or as a basis for distinguishing uncomplicated from adverse outcomes. Fourth, the cohort included different anatomical injury locations and variations in surgical repair according to tear location (anchor reinforcement vs no anchor fixation), which may have contributed to heterogeneity. Fifth, the study population consisted exclusively of young male professional football players, limiting the generalizability of these findings to other populations undergoing proximal hamstring surgery, particularly older patients and recreational athletes. Finally, electrophysiological studies were not performed, preventing confirmation of the denervation-like MRI findings.

In conclusion, serial MRI in this small cohort of young male professional football players with an uncomplicated clinical course after surgical repair of complete tears of the proximal hamstring musculotendinous complex demonstrated that postoperative MRI abnormalities evolve at different rates during the first 4 months. Scar maturation may coexist with residual intratendinous clefts, tendinous angulation, altered muscle contour, edema-like signal, and denervation-like signal. Therefore, persistent postoperative MRI abnormalities should not, in isolation, be considered evidence of failed or delayed healing. Recognition of this temporal postoperative MRI appearance may help musculoskeletal radiologists avoid overinterpretation of residual abnormalities during tendon remodeling. MRI examinations obtained before postoperative exacerbation

demonstrated extensive, prominent intratendinous clefts that were markedly hyperintense on PD-FS images, intratendinous cavities, immature scar, and persistent interstitial edema-like signal; however, these exploratory observations require validation in larger prospective cohorts before they can be used to distinguish uncomplicated from adverse postoperative healing.

Supplementary information The online version contains supplementary material available at https://doi.org/10.1007/s00256-026-05414-w.

Author contribution SM, JI: Conceptualization, study design, MRI image analysis, data interpretation, preparation of figures, manuscript drafting, and critical revision of the manuscript. PP, AC: Study design, Independent MRI image analysis and manuscript draft. XA, RP: Study design, manuscript drafting, and critical revision of the manuscript. XV, XY, IM: Clinical follow-up and critical revision of the manuscript. JP, MA, LL: Surgical treatment of the patients, clinical follow-up, and critical revision of the manuscript. CP, AK, GR: Study conception, supervision, data interpretation, and critical revision of the manuscript. All authors reviewed and approved the final version of the manuscript.

Funding This research received no specific grant from any funding agency in the public, commercial, or not-for-profit sectors.

Data availability The datasets generated and/or analyzed during the current study are not publicly available due to the confidentiality of professional athletes' medical data but are available from the corresponding author on reasonable request, subject to applicable ethical and institutional requirements.

Declarations

Ethics approval and consent to participate This study was approved by the Local Ethics Committee of Barça Innovation Hub and the Sports Medical Department and was conducted in accordance with the Declaration of Helsinki and its later amendments. Written informed consent was obtained from all participants.

Conflict of interest The authors declare no competing interests.

References

1. Ekstrand J, Hägglund M, Waldén M. Epidemiology of muscle injuries in professional football (soccer). Am J Sports Med. 2011;39(6):1226–32.
2. Pedret C, Mechó S, Ahmad G, Rodas G, Balius R. A new anatomical approach to T-junction hamstring injuries. Sports Med. 2026;56(4):1035–42.
3. Ekstrand J, Bengtsson H, Waldén M, Davison M, Khan KM, Hägglund M. Hamstring injury rates have increased during recent seasons and now constitute 24% of all injuries in men's professional football: the UEFA Elite Club Injury Study from 2001/02 to 2021/22. Br J Sports Med. 2022;57(5):292–8.
4. Bramah C, Rhodes S, Clarke-Cornwell A, et al. Sprint running mechanics are associated with hamstring strain injury: a 6-month prospective cohort study of 126 elite male footballers. Br J Sports Med. 2025. https://doi.org/10.1136/bjsports-2024-108600.
5. Yanguas J, Pruna R, Puigdellívol J, Mechó S. Clinical and imaging aspects of assessment and management of proximal long head biceps femoris injury (free-tendon and myotendinous junction injuries). A report of two cases. Apunts Med Esport. 2017;52(194):79–82.
6. Askling C, Saartok T, Thorstensson A. Type of acute hamstring strain affects flexibility, strength, and time to return to pre-injury level. Br J Sports Med. 2006;40(1):40–4.
7. Valle X, Mechó S, Alentorn-Geli E, Järvinen TAH, Lempainen L, Pruna R, et al. Return to play prediction accuracy of the MLG-R classification system for hamstring injuries in football players: a machine learning approach. Sports Med. 2022;52(9):2271–82.
8. Pedret C. Hamstring muscle injuries: MRI and ultrasound for diagnosis and prognosis. J Belg Soc Radiol. 2021;105(1):91.
9. Looney AM, Day HK, Comfort SM, Donaldson ST, Cohen SB. Proximal hamstring ruptures: treatment, rehabilitation, and return to play. Curr Rev Musculoskelet Med. 2023;16(3):103–13.
10. van der Made AD, Peters RW, Verheul C, Smithuis FF, Reurink G, Moen MH, et al. Proximal hamstring tendon avulsions: comparable clinical outcomes of operative and non-operative treatment at 1-year follow-up using a shared decision-making model. Br J Sports Med. 2022;56(6):340–8.
11. Allahabadi S, Salazar LM, Obioha OA, Fenn TW, Chahla J, Nho SJ. Hamstring injuries: a current concepts review: evaluation, nonoperative treatment, and surgical decision making. Am J Sports Med. 2024;52(3):832–44. https://doi.org/10.1177/03635465231164931.
12. Vega JF, Cervantes JE, Hu EY, Nho SJ. Proximal hamstring repair: an overview of anatomy, indications, and techniques. J Cartil Joint Preserv. 2025;5:100248. https://doi.org/10.1016/j.jcjp.2025.100248.
13. Degen RM. Proximal hamstring injuries: management of tendinopathy and avulsion injuries. Curr Rev Musculoskelet Med. 2019;12:138–46.
14. Sheean AJ, Arner JW, Bradley JP. Proximal hamstring tendon injuries: diagnosis and management. Arthroscopy. 2021;37:435–7.
15. Moatshe G, Chahla J, Vap AR, Ferrari MB, Sanchez G, Mitchell JJ, et al. Repair of proximal hamstring tears: a surgical technique. Arthrosc Tech. 2017;6:e311.
16. Lempainen L, Kosola J, Orava S. Proximal hamstring repair/reinsertion: open surgery technique. In: Bonin N, Amendola A, Bellemans J, MacDonald S, Maffulli N, editors. Hip preservation surgery: open, arthroscopic, and endoscopic techniques. Berlin: Springer; 2020. p. 271–7.
17. Jokela A, Stenroos A, Kosola J, Valle X, Lempainen L. A systematic review of surgical intervention in the treatment of hamstring tendon ruptures: current evidence on the impact on patient outcomes. Ann Med. 2022;54(1):978–88.
18. Forlizzi JM, Nacca CR, Shah SS, et al. Acute proximal hamstring tears can be defined using an imaged-based classification. Arthrosc Sports Med Rehabil. 2022;4(2):e653–9.
19. Sgustav C, Lacheta L, Stöckle U, Akgün D, Geisel D, Park HU, et al. Clinical and magnetic resonance imaging outcome after proximal hamstring tendon repair at mean 3 years follow-up. Arch Orthop Trauma Surg. 2025;145(1):130.
20. Belk JW, Kraeutler MJ, Mei-Dan O, Houck DA, McCarty EC, Mulcahey MK. Return to sport after proximal hamstring tendon repair: a systematic review. Orthop J Sports Med. 2019;7(6):2325967119853218.
21. Isern-Kebschull J, Mechó S, Pedret C, Pruna R, Alomar X, Kassarjian A, et al. Muscle healing in sports injuries: MRI findings and proposed classification based on a single institutional experience and clinical observation. Radiographics. 2024;44(8):e230147.
22. Mechó S, Isern-Kebschull J, Alomar X, Wong M, Congo A, Pedret C. Muscle healing in sports injuries. Aspetar Sports Med J. 2025;14:94–101.
23. Baldock J, Wright S, McNally E, Wedatilake T. Intratendinous hamstring injuries: sequential MRIs as a tool to reduce the risk of reinjury in elite sport. BMJ Case Rep. 2021;14(11):e241365.

24. Isern-Kebschull J, Pedret C, Mechó S, Pruna R, Alomar X, Yanguas X, et al. MRI findings prior to return to play as predictors of reinjury in professional athletes: a novel decision-making tool. Insights Imaging. 2022;13(1):203.
25. Finch CF, Cook J. Categorising sports injuries in epidemiological studies: the subsequent injury categorisation (SIC) model to address multiple, recurrent and exacerbation of injuries. Br J Sports Med. 2014;48(17):1276–80.
26. Lempainen L, Kosola J, Pruna R. Central tendon injuries of hamstring muscles. Orthop J Sports Med. 2018;6(2):2325967118755992.
27. Chhabra A, Andreisek G, Soldatos T, et al. MR neurography: past, present, and future. AJR Am J Roentgenol. 2011;197:583–91.
28. Pollock N, James SLJ, Lee JC, Chakraverty R. British athletics muscle injury classification: a new grading system. Br J Sports Med. 2014;48(18):1347–51.
29. Valle X, Alentorn-Geli E, Tol JL, Hamilton B, Garrett WE, Pruna R, et al. Muscle injuries in sports: a new evidence-informed and expert consensus-based classification with clinical application. Sports Med. 2017;47:1241–53.
30. Järvinen TA, Järvinen TL, Kääriäinen M, Kalimo H, Järvinen M. Muscle injuries: biology and treatment. Am J Sports Med. 2005;33(5):745–64.
31. Järvinen TA, Järvinen M, Kalimo H. Regeneration of injured skeletal muscle after the injury. Muscles Ligaments Tendons J. 2014;3(4):337–45.
32. Kalimo H, Rantanen J, Järvinen M. Muscle injuries in sports. Baillieres Clin Orthop. 1997;2:1–24.
33. Isern-Kebschull J, Mechó S, Pruna R, et al. Sports-related lower limb muscle injuries: pattern recognition approach and MRI review. Insights Imaging. 2020;11(1):108.
34. Chianca V, Zappia M, Oliva F, Del Buono A, Maffulli N. Postoperative MRI and US appearance of the Achilles tendon. J Ultrasound. 2020;23:387–95.
35. Reurink G, Goudswaard GJ, Tol JL, Almusa E, Moen MH, Weir A, et al. MRI observations at return to play of clinically recovered hamstring injuries. Br J Sports Med. 2014;48:1370–6.
36. Fleckenstein JL, Watumull D, Conner KE, Ezaki M, Greenlee RG, Bryan WW. Denervated human skeletal muscle: MR imaging evaluation. Radiology. 1993;187:213–8.
37. Guttmann E. Neurotrophic relations. Annu Rev Physiol. 1976;38:177–216.
38. Lin Y, Sahr M, Lan R, Nguyen J, Tan ET, Sneag DB. MRI findings correlate with difficult dissection during proximal hamstring repair and with postoperative sciatica. Skeletal Radiol. 2024;53:2449–57.

Publisher's Note Springer Nature remains neutral with regard to jurisdictional claims in published maps and institutional affiliations.

Springer Nature or its licensor (e.g. a society or other partner) holds exclusive rights to this article under a publishing agreement with the author(s) or other rightsholder(s); author self-archiving of the accepted manuscript version of this article is solely governed by the terms of such publishing agreement and applicable law.